J. Fluid Mech. (1996), *vol.* 324, *pp.* 135–161
Copyright © 1996 Cambridge University Press

Oscillating flow of a heat-conducting fluid in a narrow tube

By LUC BAUWENS

The University of Calgary, Department of Mechanical Engineering, Calgary, AB T2N 1N4, Canada

e-mail: bauwens@acs.ucalgary.ca

(Received 11 January 1995 and in revised form 26 April 1996)

Thermoacoustic refrigeration occurs in periodic flow in a duct with heat transfer within the fluid and to the tube. This study considers the periodic limit cycle with large pressure oscillations that is obtained in a tube when prescribed, phase-shifted, periodic velocities at the tube ends, at frequencies lower than acoustic eigenmodes, sweep a length comparable to the tube length. The temperature differences between the two ends are of arbitrary magnitude, heat transfer in the transverse direction within the fluid is assumed to be very effective and the thermal mass of the wall is large. The geometry is two-dimensional, axisymmetric, and conduction is accounted for, not only in the fluid, but also with and within the tube wall. A perturbation solution valid in a local near-isothermal limit determines the equilibrium longitudinal temperature profile that is reached at the periodic regime, the pressure field including longitudinal gradients, and the longitudinal enthalpy flux. Results are presented for tubes open at both ends and also with one end closed. In the latter case, a singularity occurs in the temperature at the closed end, with behaviour identical to Rott's result for acoustic flow with small pressure amplitude. Other new results obtained for tubes open at both ends show that when velocities at both ends are in opposite phase, internal singularities in the temperature profiles may occur.

1. Introduction

Thermoacoustic phenomena include Taconis waves (Taconis *et al.* 1949), the Hartmann–Sprenger tube (Sprenger 1954), acoustic refrigeration (Swift 1988), pulse-tube refrigeration (Gifford & Longsworth 1964, 1966; Radebaugh 1990) and thermal-lag engines (West 1993). The first account of conduction in acoustics is due to Kirchhoff (1868), whose theory was included in Lord Rayleigh's (1896) book and later picked up by Kramers (1949) to explain the phenomena noted by Taconis *et al.* (1949). Rott (1969, 1973), Rott & Zouzoulas (1976), Zouzoulas & Rott (1976), and Müller & Rott (1983) then consolidated this and provided definitive treatment of near-resonant thermally driven acoustic flow.

Self-sustained oscillations known as Taconis waves occur in cryogenic storage, in a tube with a closed end exposed to ambient temperature and an open end inside a liquid helium bath. The conditions under which these oscillations develop spontaneously can be found by linear stability analysis about a prescribed temperature distribution, which yields a dispersion relation. The locus of purely imaginary frequencies in parameter space determines the stability boundary. This model is acoustic; the frequencies are acoustic eigenmodes for the specified temperature profile.

Also in the small amplitude near-resonant acoustic limit, Merkli & Thomann (1975)

studied heat streaming in thermoacoustics. Thomann (1976) and Rott (1975) evaluated the enthalpy flux, respectively in the case of Stokes layers larger and smaller than the tube diameter. Both cases, of narrow and wide tubes, were included in Rott's final 1984 paper. In contrast with the present one, these studies considered prescribed longitudinal temperature distributions, away from equilibrium, hence a non-uniform enthalpy flux along the tube. But then, as the amplitude of the motion increases, the wall temperature evolves in response to the imbalance in heat transfer with the fluid, until a limit cycle is reached and the enthalpy flux becomes uniform. Meanwhile, the amplitude of the motion and the pressure oscillations increase, nonlinear interactions become significant and linearized analysis is no longer valid at the limit cycle.

The present study is concerned with a situation akin to that limit cycle, which arises in the context of oscillating flows with large pressure fluctuations and large energy exchanges in the presence of large absolute temperature differences, and leads to a different problem formulation: for prescribed motions at the tube ends, to find the *equilibrium* longitudinal temperature distribution at the stationary periodic regime, *when the energy transfers are thus balanced.* The present analysis successfully determines the limit cycle where Rott's approach fails, because of one key difference in the scaling of the problem: this study considers frequencies lower than acoustics, or in other words, non-acoustically resonant flow. It encompasses situations where it is the forced motion at both ends of the tube that determines the frequency, which is thus no longer an eigenvalue but a parameter belonging in the problem statement, and can thus be lower than the resonant modes. While the low-frequency motion can still realistically be described as a low-Mach-number motion, in contrast with Rott's small displacements, the amplitude is now comparable to the tube length. Finally, if the motion sweeps a large fraction of the tube length, then the mass of fluid in the tube experiences large fluctuations, so that temporal pressure oscillations now have a magnitude comparable to the mean pressure.

Even for Taconis waves, non-acoustic models have been suggested (Rudman 1994). Experiments (Gu & Timmerhaus 1994) point to wavelengths much larger than the tube length. Thus, even then, the physically relevant frequencies may often be much lower than the acoustic frequencies considered in the previous studies, and the current theory may still be applicable.

Additionally, this study is restricted to diameters smaller than the heat penetration depth and to the case of a wall with large thermal mass. Under these two conditions, the temperature of the fluid is nearly uniform in the transverse direction, and time independent. This leads to a perturbation scheme based upon the diameter being small compared to the thermal boundary layer, and the thermal mass of the gas being small compared to the wall's. The leading-order temperature varies then only along the tube length, but remains arbitrary in the leading-order problem. (In Rott's model, transverse temperature fluctuations are small too, but for a different reason: the motion is of sufficiently small amplitude so that, over the length swept by the fluid, fluctuations due to the longitudinal wall temperature gradient are small.)

In the periodic regime, the net enthalpy flux over the full period is necessarily uniform. In the perturbation solution, periodicity of the higher-order temperature fluctuations requires uniformity of the net total enthalpy flux, including conduction in the wall, which leads to a condition that ultimately determines the leading-order temperature profile. Once that profile is determined, a complete solution is readily found, including the enthalpy flux, the axial and radial velocities, the pressure fluctuation and the pressure gradient.

Potential applications of this theory include tubular regenerators, basic pulse-tube

refrigeration, gas springs (Mirels 1994*a*) and, generally, heat exchangers and other cases of narrow flow passages subjected to large pressure oscillations in which the pressure gradients are relatively small compared with the temporal fluctuation. While application to the basic pulse-tube is only valid in the narrow-tube limit, it also has some advantages compared with small-amplitude linear models (Lee *et al.* 1995; Mirels 1994*b*) which do not suffer from the narrow-tube limitation but instead, assume a small temperature amplitude, a small pressure fluctuation and a small sweep. Both approaches are complementary in that they cover different regions in the parameter space and that they suffer from different limitations. The current analysis is not applicable to resonant pulse-tube refrigerators, which are more accurately described by Rott's linearized theory, nor to orifice-type pulse-tube refrigerators, which are typically constructed with a large diameter, avoiding as much as possible true thermoacoustic effects, and which can then be analysed as a variant of the Stirling cycle (Kittel 1992). The energy fluxes in a large tube can be predicted using an adiabatic model, such as that of Storch & Radebaugh (1988).

The main goal here is development of the low-frequency theory, which targets a generic case in which velocities are prescribed at both ends of the tube. Additionally, to show the power of the theory, two cases are solved in some detail below. The first one considers a tube closed at one end, in which case all leading-order entropy and energy exchanges vanish. In the absence of a heat exchanger at the closed end, this system turns into a degenerate case of a pulse-tube refrigerator. The second case considers non-zero velocities at both ends, yielding a non-zero leading-order entropy flux, typical of the Stirling cycle.

Remarkably, in the case of a tube closed at one end, and neglecting longitudinal conduction in the wall, the same singular behaviour as noted by Rott (1984) in the temperature profile is obtained at the closed end. For flows that are strictly of opposite phase at the ends, the temperature profile also exhibits a singularity, but at a location inside the tube where velocity remains zero.

Finally, it is interesting to compare the results obtained here, which are based upon a full solution for the complete velocity field, the pressure field including viscous gradients and the two-dimensional temperature field, to the results produced by a similar one-dimensional nearly isothermal model based upon empirical friction and convection correlations (Bauwens 1995). The comparison shows that even in the laminar limit, and using the exact Nusselt number for tubes, the one-dimensional model does not quite yield the correct solution for the contribution to the enthalpy flux due to pressure oscillations. Thus, strictly speaking, the one-dimensional model is only valid for systems open to a large pressure reservoir so that pressure remains uniform.

2. The near-isothermal model

The current model is near-isothermal, using the meaning of the word from the heat engine literature, in which context the basic idea underlying the near-isothermal model originally arose. Thus, a device in which local temperatures are time independent is characterized as isothermal even though the spatial, longitudinal temperature gradients may be large. Strictly speaking, it is isothermal only locally. This contrasts with the large industrial regenerators studied by Hausen (1929) and Schmidt & Willmott (1981), which are nearly isothermal globally, in which the pressure fluctuations are small and the blow time is considerably larger than the residence time, and which are well-described by a constant-density model.

The near-isothermal idea was originally proposed by Rea & Smith (1967), who

mentioned applicability to pulse-tubes also, and by Qvale & Smith (1969), and independently by Bauwens (1995). If heat transfer is very efficient and the thermal mass of the wall or matrix is large, fluid and wall are then at approximately the same time-independent temperature. Nearly all the enthalpy of the fluid entering the tube or regenerator is returned when the fluid returns. In the limit, if both the heat transfer coefficient and the thermal mass are infinite, the ideal isothermal model due to Schmidt (1871; see also Urieli & Berchowitz 1984) is obtained.

If the system were truly isothermal, and with infinite thermal mass, its temperature would never change. Thus, the longitudinal temperature would be determined at all times by its initial value, and any arbitrary initial temperature distribution would be a valid temperature profile at all times. However, even for very small departures from strict isothermality, the stationary, periodic regime can no longer be maintained for arbitrary temperature profiles. In the stationary regime, the total net enthalpy flux including conduction in the wall over one full period is necessarily uniform along the length, otherwise the temperatures do not return to their initial value at the end of the period, and they cannot be periodic functions of time.

Qvale & Smith observed that the temperature profile is ultimately determined by longitudinal uniformity of the enthalpy flux. They in effect represented temperatures by what amounts to a uniform spanwise and time-independent leading-order approximation, plus a small perturbation which varies with time and along the transverse direction, but they did not actually solve for temperature. Instead, they arbitrarily assumed a fourth-order polynomial expression, the lowest order allowing for equality of the enthalpy flux at both ends – but not elsewhere along the regenerator length. Only recently has a full one-dimensional solution for the temperature profile appeared (Bauwens 1995). A related harmonic regenerator model (based upon a scaling and a perturbation scheme similar to Rott's), in which the longitudinal equilibrium temperatures are determined by enthalpy flux uniformity, was recently proposed by Swift & Ward (1995).

Regenerators are typically made of screens or other irregular material, with complicated topology, which often cannot be characterized in detail, so that, even at the low Reynolds numbers typical of regenerators, a full three-dimensional solution resolving the temperature, pressure and velocity fields, is not feasible. Instead, the flow is approximated as one-dimensional in space (and time dependent). However, then, velocity and temperature are no longer resolved in the transverse direction so that viscous losses and heat transfer can no longer be determined according to the true physical models. Instead, heat transfer between fluid and matrix and viscous losses are evaluated using an empirical convection coefficient and an empirical friction factor. But empirical correlations giving the Nusselt or Stanton number and the friction factor as functions of the Reynolds number are measured in steady flow experiments, hence, unavoidably, uniform pressure. This inconsistency is unavoidable in one-dimensional models, whether approximate, semi-analytical, or fully discretized numerical codes (Gary & Radebaugh 1989; Gedeon 1986; Bauwens & Mitchell 1991).

The idea underlying the nearly isothermal one-dimensional regenerator model also applies to the two-dimensional flow in a tube that is of interest here. Additionally, in the two-dimensional solution, transverse gradients can be fully resolved. The effect of viscous stresses on the pressure gradient is thus determined using the viscosity law, and heat transfer is based upon transverse heat diffusion according to Fourier's law. Consequently, the two-dimensional tube solution avoids the main weakness of one-dimensional regenerator models, namely the empirical friction and convection models, albeit for a simpler topology.

3. Two-dimensional problem and magnitude assumptions

A periodic solution for the flow and temperature field in a round tube is sought, with heat transfer between the fluid and the tube. At each end, the volumetric flow is a known periodic function of time, the velocity is uniform spanwise and the known temperature of the fluid is normally not the same at both ends. The mean pressure is known. The outer tube wall is thermally insulated. The left and right faces of the tube are at the temperature of the entering fluid. The fluid is an ideal gas with constant specific heats; its thermal conductivity and dynamic viscosity are independent of pressure but they vary with temperature.

Independent variables present in the problem are as follows: dimensions include tube length, inside radius and wall thickness. The gas is characterized by its dynamic viscosity $\mu(T)$, its thermal conductivity $k(T)$, its specific heat c_v and the specific heat ratio γ. The wall material is characterized by $(\rho_m c_m)(T)$ and $k_m(T)$. Operating parameters include the mean pressure P, the period τ, periodic velocities and fixed temperatures at both ends. These fifteen independent variables result in eleven independent dimensionless parameters (Organ 1992; Olson & Swift 1994). However, to maintain the problem symmetry, instead of using the temperature at one end as the temperature scale, an arbitrary additional parameter is introduced: a reference temperature T_{ref}. Formally, the problem now depends upon twelve dimensionless parameters.

The solution is carried out under the following assumptions:

(i) The length of the tube L is much larger than the radius R. Inside the tube, the radial coordinate r is scaled by R. In the wall, a rescaled transverse coordinate $\sigma = (R/d)r$ is used, which varies by 1 across the wall thickness d; this allows wall thicknesses of magnitudes possibly different from the inside diameter to be considered (with adjustment to Cartesian coordinates and σ from 0 to 1 if $R \gg d$).

(ii) The length swept by the fluid motion is of magnitude comparable with the tube length. Longitudinal velocities are thus of magnitude L/τ, τ being the period, and L, the tube length. In particular the dimensionless velocities U_L and U_R at the boundaries are of order unity.

(iii) The heat penetration depth in the gas is large compared to the tube diameter. Equivalently, the time scale for transverse conduction in the fluid is smaller than the period:

$$\epsilon = \frac{R^2}{\alpha_{ref}\tau} \ll 1, \tag{1}$$

in which α_{ref}, the thermal diffusivity of the fluid, is evaluated at the mean pressure and at the reference temperature. Equation (1) ensures that small transverse temperature gradients are sufficient for transferring to the wall the energy advected by the longitudinal flow.

(iv) If, furthermore, the useful thermal mass of the wall is larger than the thermal mass of the fluid, then the amplitude of the temperature fluctuation is also small, ensuring that the flow is nearly isothermal. If the entire wall thickness contributes to the thermal mass (see Assumption (v)), then this is expressed as follows, in which the fluid density ρ is evaluated at the reference conditions, and the wall material properties are evaluated at T_{ref}:

$$\delta = \frac{\rho c_p R}{\rho_m c_m d} \ll 1. \tag{2}$$

(v) The analysis is restricted to the case where the entire wall thickness contributes

to the thermal mass. The parameter $a(T)$ defined as follows is then at most of order unity:

$$a(T) = \frac{\alpha_m \tau}{d^2}, \tag{3}$$

where α_m is the thermal diffusivity of the wall material.

(vi) Longitudinal conduction in the wall is, at most, of the same magnitude as the enthalpy flux due to the oscillating flow. In many cases, longitudinal conduction will not be significant. Still, transverse conduction in the wall is crucial to acoustic refrigeration. It is useful to verify that it is indeed possible to have adequate transverse conduction, while longitudinal conduction remains insignificant.

The condition under which longitudinal conduction in the wall is small compared to the energy convected by the fluid is $k_m T_{ref} Rd/L \ll \rho u c_p T_{ref} R^2$, or $\tau\alpha_m/L^2 \ll \delta$. More precisely, the analysis targets the case in which heat leakage in the wall is, at most, as important as the loss due to transverse conduction in the fluid, in which case the ratio of wall conduction leakage to convection in the gas is of order ϵ. To that effect, a dimensionless parameter $b(T)$ which is at most of order unity is introduced:

$$\frac{\tau\alpha_m}{L^2} = a\frac{d^2}{L^2} = b(T)\,\delta\epsilon. \tag{4}$$

(vii) Longitudinal conduction in the fluid is negligible, which requires $R/L \ll \epsilon$.

(viii) Finally, the study is limited to the case where spatial pressure gradients are of a magnitude smaller than the amplitude of the temporal pressure fluctuation, which is comparable to the mean pressure, thus $\mu L^2/\tau R^2 \ll P$. For μ at the reference temperature,

$$M^2 = \frac{L^2}{\tau^2 c_{ref}^2} \ll \frac{R^2}{Pr_{ref}\alpha_{ref}\tau} = Re_{ref} R/L = \epsilon/Pr_{ref}. \tag{5}$$

In (5), the reference Mach number M is based upon the velocity scale L/τ and the speed of sound at the reference temperature T_{ref}. Pr_{ref} is the Prandtl number at the reference temperature, and Re_{ref} the corresponding Reynolds number. And because of Assumption (iii), $R^2/\alpha\tau = \epsilon \ll 1$, so that $Pr_{ref} M^2 \ll \epsilon \ll 1$.

This assumption, more restrictive than taking $M \ll 1$, can be explained in an alternative way. Equation (5) requires that the tube length be less than the wavelength L_{crit} of Rott's solution in the case of a thick Stokes layer, which was shown by Thomann (1976) to be equal to $\tau c\epsilon^{1/2}$.

Summarizing, four of the twelve parameters which the dimensionless problem depends upon are small:

$$\epsilon = \frac{R^2}{\alpha\tau}, \quad M = \frac{L}{\tau c_{ref}}, \quad \delta = \frac{\rho c_p R}{\rho_m c_m d}, \quad R^2/L^2.$$

The four small parameters can be varied independently, except that $Pr_{ref} M^2 \ll \epsilon$ and $R/L \ll \epsilon$. The other eight parameters, $\mu(T)/\mu_{ref}$, γ, U_L, U_R, T_L, T_R, $a(T)$ and $b(T)$ are of order unity.

4. Dimensionless periodic boundary value problem

A periodic solution $u(x, r, t)$, $v(x, r, t)$, $p(x, r, t)$, $\rho(x, r, t)$, $T(x, r, t)$ and $T_m(x, \sigma, t)$ is sought, with period 1, satisfying (6) below. The velocities u and v, and the thermodynamic state p, ρ and T are defined on a cylindrical domain (x, r) determined

by $x \in [0, 1]$ and $r \in (0, 1]$. T_m is defined on $x \in [0, 1]$ and $\sigma \in [R/d, 1 + R/d]$. The boundary conditions are shown on figure 1.

The problem has been made dimensionless by scaling x by the tube length L, the radial coordinate r by the radius R, the radial coordinate σ by the wall thickness d, time by the period τ, axial velocity u by L/τ, radial velocity v by R/τ, pressure by the mean pressure P, temperature, by an arbitrary temperature scale T_{ref}, and density, by its value at P and T_{ref}:

$$M^2\rho\left(\frac{\partial u}{\partial t}+u\frac{\partial u}{\partial x}+v\frac{\partial u}{\partial r}\right)=-\frac{1}{\gamma}\frac{\partial p}{\partial x}+\frac{Pr_{ref}M^2}{\epsilon}\left\{\frac{1}{r}\frac{\partial\left(\frac{\mu(T)}{\mu_{ref}}r\frac{\partial u}{\partial r}\right)}{\partial r}+O(R^2/L^2)\right\}, \tag{6a}$$

$$M^2\frac{R^2}{L^2}\rho\left(\frac{\partial v}{\partial t}+u\frac{\partial v}{\partial x}+v\frac{\partial v}{\partial r}\right)=-\frac{1}{\gamma}\frac{\partial p}{\partial r}+O\left(\frac{Pr_{ref}M^2}{\epsilon}\frac{R^2}{L^2}\right), \tag{6b}$$

$$\frac{\partial\rho}{\partial t}+\frac{\partial(\rho u)}{\partial x}+\frac{1}{r}\frac{\partial(\rho v r)}{\partial r}=0, \tag{6c}$$

$$\epsilon\left(\frac{1}{\gamma}\frac{\partial(\rho T)}{\partial t}+\frac{1}{r}\frac{\partial(rvp)}{\partial r}+\frac{\partial(up)}{\partial x}\right)+O\left(\epsilon M^2\frac{\gamma-1}{\gamma}\right)-O\left(Pr_{ref}M^2\frac{\gamma-1}{\gamma}\right)$$

$$=\frac{1}{r}\frac{\partial\left(r\frac{k(T)}{k_{ref}}\frac{\partial T}{\partial r}\right)}{\partial r}+\frac{R^2}{L^2}\frac{\partial}{\partial x}\left(\frac{k(T)}{k_{ref}}\frac{\partial T}{\partial x}\right), \tag{6d}$$

$$\frac{\partial T_m}{\partial t}=\delta\epsilon\frac{\partial}{\partial x}\left(b\frac{\partial T_m}{\partial x}\right)+\frac{1}{\sigma}\frac{\partial\left(\sigma a\frac{\partial T_m}{\partial\sigma}\right)}{\partial\sigma}, \tag{6e}$$

$$p=\rho T, \tag{6f}$$

$$u(0, r, t)=U_L(t), \quad v(0, r, t)=0, \tag{6g,h}$$

$$T(0, r, t)=T_m(0, r, t)=T_L, \tag{6i,j}$$

$$u(l, r, t)=U_R(t), \quad v(l, r, t)=0, \tag{6k,l}$$

$$T(l, r, t)=T_m(l, r, t)=T_R, \tag{6m,n}$$

$$u(x, l, t)=0, \quad v(x, l, t)=0, \tag{6o,p}$$

At the gas–tube interface,

$$T(x, r=l, t)=T_m\left(x, \sigma=\frac{R}{d}, t\right), \quad \delta\frac{k(T)}{k_{ref}}\frac{\partial T}{\partial r}\bigg|_{r=1}=\epsilon a\frac{\partial T_m}{\partial\sigma}\bigg|_{\sigma=R/d}, \tag{6q,r}$$

$$\frac{\partial T_m}{\partial\sigma}=0 \quad \text{at the outer tube wall, } \sigma=1+\frac{R}{d}, \tag{6s}$$

$$\int_0^1 p(1/2, 0, t)\,\mathrm{d}t=1. \tag{6t}$$

Equations (6*a*) and (6*b*) are the momentum equations; (6*c*) is continuity; (6*d*) and (6*e*) are the energy equations, respectively for the fluid and for the wall; (6*f*) is the equation

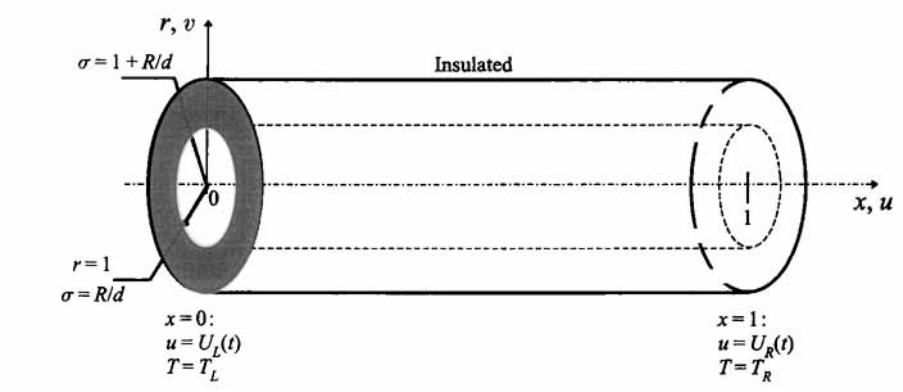

FIGURE 1. Solution domain, coordinates and boundary conditions.

of state. (The energy equation for the fluid, (6*d*), is the total energy equation, including thermal and kinetic energy. In the thermal energy equation, the contribution of order ϵ would be

$$\frac{1}{\gamma}\frac{\partial(\rho T)}{\partial t}+\frac{1}{\gamma}\nabla\cdot(\boldsymbol{u}p)+\frac{\gamma-1}{\gamma}p\nabla\cdot\boldsymbol{u}.$$

This is equal to the term of order ϵ in (6*d*), minus $[(\gamma-1)/\gamma]\boldsymbol{u}\cdot\nabla p$ which, in view of the momentum equation, is of order M^2 and results in the second (kinetic energy) and third (viscous heating) terms of (6*d*).) Equations (6*g*)–(6*s*) are the boundary conditions; in (6*g*, *k*), $U_L(t)$ and $U_R(t)$ are known periodic functions with period 1. Finally, the auxiliary condition (6*t*), necessary for well-posedness, sets the dimensionless mean pressure equal to 1.

5. Perturbation solution

5.1. *Perturbation series*

According to (5), $Pr_{ref}M^2/\epsilon \ll 1$. Consequently, the largest independent small parameters that appear in the problem are ϵ, δ, R^2/L^2 and $Pr_{ref}M^2/\epsilon$. To the magnitudes of interest, the solution to orders depending upon R^2/L^2 remains fully decoupled and has no impact on the solution being sought. Furthermore, no assumptions have been made regarding the relative magnitudes of these parameters, and δ only appears in equations that involve T_m: hence the perturbation series:

$$p = p_0+\epsilon p_{11}+\frac{Pr_{ref}M^2}{\epsilon}p_{12}+\epsilon^2 p_{21}+\ldots, \tag{7a}$$

$$\rho = \rho_0+\epsilon\rho_{11}+\frac{Pr_{ref}M^2}{\epsilon}\rho_{12}+\epsilon^2\rho_{21}+\ldots, \tag{7b}$$

$$T = T_0+\epsilon T_{11}+\delta T_{13}+\epsilon^2 T_{21}+\ldots, \tag{7c}$$

$$T_m = T_{m0}+\epsilon T_{m11}+\delta T_{m13}+\epsilon^2 T_{m21}+M^2 T_{m22}+\delta\epsilon T_{m23}+\ldots, \tag{7d}$$

$$u = u_0+\epsilon u_{11}+\frac{Pr_{ref}M^2}{\epsilon}u_{12}+\epsilon^2 u_{21}+\ldots, \tag{7e}$$

$$v = v_0+\epsilon v_{11}+\frac{Pr_{ref}M^2}{\epsilon}v_{12}+\epsilon^2 v_{21}+\ldots. \tag{7f}$$

The two key effects of R^2/L^2 being small are the usual ones: the transverse pressure gradient is smaller than the longitudinal pressure gradient, and longitudinal diffusion

of momentum and heat is negligible compared with transverse diffusion. This affects the boundary conditions, which have to be expanded in perturbation series also, and be ascribed to the term of the appropriate magnitude. The original heat equation was elliptic in x and thus supported, in principle, temperature boundary conditions at both ends. But because longitudinal conduction is neglected in the leading-order energy equation for the fluid, the leading-order problem is now hyperbolic in x, and it can only support one boundary condition for temperature, at inlet but not at outlet. This is consistent with the fact that, physically, it is possible to supply fluid at a given temperature, but the temperature at which the fluid leaves the system is determined by heat transfer inside. In the current problem, however, the flow oscillates, and each end operates as an inlet during part of the period. A temperature boundary condition can only be enforced, at each end, whenever the velocity at that end is in the direction entering the tube.

5.2. *Leading order problem*

Expressing pressure, temperatures, density and velocities by the perturbation series (7) in (6), and collecting the leading-order terms, one obtains

$$\frac{\partial p_0}{\partial x} = 0, \quad \frac{\partial p_0}{\partial r} = 0, \quad \frac{\partial \rho_0}{\partial t} + \frac{\partial(\rho_0 u_0)}{\partial x} + \frac{1}{r}\frac{\partial(\rho_0 v_0 r)}{\partial r} = 0, \tag{8a–c}$$

$$\frac{1}{r}\frac{\partial\left(r\dfrac{k(T_0)}{k_{ref}}\dfrac{\partial T_0}{\partial r}\right)}{\partial r} = 0, \quad \frac{\partial T_{m0}}{\partial t} = \frac{1}{\sigma}\frac{\partial(\sigma a\,\partial T_{m0}/\partial\sigma)}{\partial\sigma}, \tag{8d, e}$$

$$p_0 = \rho_0 T_0, \quad u_0(0, r, t) = U_L(t), \quad v_0(0, r, t) = 0, \tag{8f–h}$$

$$T_0(0, r, t) = T_{m0}(0, r, t) = T_L \quad \text{when} \quad U_L(t) > 0, \tag{8i, j}$$

$$u_0(l, r, t) = U_R(t), \quad v_0(l, r, t) = 0, \tag{8k, l}$$

$$T_0(l, r, t) = T_{m0}(l, r, t) = T_R \quad \text{when} \quad U_R(t) < 0, \tag{8m, n}$$

$$u_0(x, l, t) = 0, \quad v_0(x, l, t) = 0, \quad T_0(x, r = l, t) = T_{m0}(x, \sigma = R/d, t), \tag{8o–q}$$

$$\left.\frac{\partial T_0}{\partial r}\right|_{r=1} = 0, \quad \left.\frac{\partial T_{m0}}{\partial \sigma}\right|_{\sigma=R/d} = 0, \quad \left.\frac{\partial T_{m0}}{\partial \sigma}\right|_{\sigma=1+R/d} = 0, \tag{8r–t}$$

$$\int_0^1 p_0\,\mathrm{d}t = 1. \tag{8u}$$

This set of equations leads to the classical Schmidt isothermal solution. This problem can be separated into the wall problem and the fluid problem.

The wall problem is parabolic in t and σ, with x appearing only as a parameter. The unique periodic or stationary solution to (8*e*) with the boundary conditions given by (8*s*, *t*) is $T_{m0} = T_{m0}(x)$ defined by the initial conditions, which are arbitrary so far.

For conduction in the gas, the only solution to (8*d*) with T_0 finite at $r = 0$ is $T_0 = T_0(x, t)$. But since at the wall–gas interface, according to (8*q*), temperature is continuous, then $T_{m0} = T_0 = T_0(x)$. Both temperatures are equal; they are time independent and uniform in r and σ; and they only depend upon the longitudinal position x. Thus, to leading order, the flow is isothermal.

Equations (8*a*) and (8*b*) indicate that the pressure p_0 depends upon time only. Next, density is replaced by its value from the state equation, $\rho_0 = p_0(t)/T_0(x)$, in the continuity equation (8*c*):

$$\frac{\mathrm{d}p_0}{\mathrm{d}t} + T_0 p_0 \frac{\partial(u_0/T_0)}{\partial x} + p_0 \frac{1}{r}\frac{\partial(v_0 r)}{\partial r} = 0. \tag{9}$$

Integrating (9) divided by T_0 over the whole tube volume, with velocities at the ends given by (8g) and (8k), and temperatures by (8i) and (8 m), it follows that

$$\frac{\mathrm{d}p_0}{\mathrm{d}t}\int_0^1 \frac{1}{T_0}\mathrm{d}x + p_0\frac{U_R}{T_R} - p_0\frac{U_L}{T_L} = 0. \tag{10}$$

Integrating (10) with respect to time over the whole period, the work done by the pressure forces at the ends is found to be related by the Carnot relationship, which is consistent with the Schmidt solution. The leading-order solution is thus fully reversible.

Integration of (10) divided by p_0 with respect to time yields a value for pressure:

$$p_0(t) = \exp\int_0^t \left(\frac{\bar{T}U_L(t)}{T_L} - \frac{\bar{T}U_R(t)}{T_R}\right)\mathrm{d}t, \tag{11}$$

$$\bar{T} = 1\Big/\int_0^1 \frac{1}{T_0(x)}\mathrm{d}x. \tag{12}$$

Since T_0 is now a function of x only, the mean temperature $\bar{T}$ defined by (12) is an absolute constant, the value of which is, however, unknown at this stage.

Leading-order pressure depends upon time only while temperature depends upon x only. The dependency of the temperature on x remains indeterminate, however. For velocities, the single equation (9) relates the two unknown velocity components u_0 and v_0.

5.3. *Problem of order* $Pr_{ref}M^2/\epsilon$

Velocities depend upon the momentum balance. To leading order, the momentum equation, (6a), resulted in pressure being spatially uniform. Indeed, the largest contribution to pressure gradients is due to viscous stresses and is of order $Pr_{ref}M^2/\epsilon$. Collecting terms of that magnitude in (6a, b), with the unknowns replaced from (7), gives

$$\frac{1}{\gamma}\frac{\partial p_{12}}{\partial x} = \frac{\mu(T_0)}{\mu_{ref}}\frac{1}{r}\frac{\partial(r\,\partial u_0/\partial r)}{\partial r}, \quad \frac{\partial p_{12}}{\partial r} = 0. \tag{13a, b}$$

It follows from (13b) that $p_{12} = p_{12}(x,t)$. Thus, integrating (13a) twice with respect to r, noting that the left-hand side is independent of r, and taking into account that velocity cannot be singular at $r = 0$, and that, from (6o), at $r = 1$, $u = 0$, one obtains

$$u_0 = \frac{\mu_{ref}}{4\gamma\mu(T_0)}\frac{\partial p_{12}}{\partial x}(r^2 - 1). \tag{14}$$

Replacing u_0 by this value in (9), multiplying by r and integrating with respect to r between 0 and 1, and taking into account that, according to (6p), $v_0 = 0$ at $r = 1$ and that also, by symmetry, $v_0 = 0$ at $r = 0$, results in

$$\frac{1}{p_0}\frac{\mathrm{d}p_0}{\mathrm{d}t} = \frac{T_0}{8\gamma}\frac{\partial\left(\dfrac{\mu_{ref}}{\mu(T_0)}\dfrac{1}{T_0}\dfrac{\partial p_{12}}{\partial x}\right)}{\partial x}. \tag{15}$$

Integrating (9) times r between 0 and r and taking (15) into account, it follows that

$$v_0 = \frac{1}{2p_0}\frac{\mathrm{d}p_0}{\mathrm{d}t}r(1 - r^2). \tag{16}$$

However, neither u_0 given by (14) nor v_0 given by (16) satisfy the boundary conditions at $x = 0$ and $x = 1$, equations (8g, h, k, l). This entry length issue can be resolved by

introducing an inner problem at each end, locally rescaling x by a factor R/L. Introducing a rescaled longitudinal coordinate X, for instance at $x = 0$, $X = (L/R)x$, and noting that within the entry length, there exists a transverse velocity of magnitude L/τ so that a rescaled transverse velocity $V = (L/R)v$ must also be introduced, the continuity equation becomes

$$\frac{R}{L}\frac{\partial \rho}{\partial t} + \frac{\partial(\rho u)}{\partial X} + \frac{1}{r}\frac{\partial(\rho V r)}{\partial r} = 0.$$

Furthermore, the leading-order pressure and temperature remain uniform in the entry region, for the same reasons as in the outer region, so that, to order ϵ (because of temperature) and R/L (because of the first term in the rescaled equation), velocity is divergence free in the entry region, while because of the rescaling the pressure gradient only would contribute to a smaller correction, of order R/L times $Pr_{ref}M^2/\epsilon$. After integration over the entire cross-section, this indicates that, up to corrections of order R/L and ϵ, the mass flow rate is uniform along the entry length.

Thus, matching the entry (inner) problem with the outer problem merely requires that the total volumetric flow at the extremity of the outer problem be equal to the total volumetric flow from the boundary condition, $(8g, k)$. This can be written as

$$\pi U_L(t) = \int_0^1 u_0(0, r, t)\, 2\pi r \, \mathrm{d}r, \tag{17}$$

$$\pi U_R(t) = \int_0^1 u_0(l, r, t)\, 2\pi r \, \mathrm{d}r. \tag{18}$$

The rescaled problem will take care of the necessary adjustments. The differences between the velocity at the end of the tube and the matching velocity at the interface between the inner, rescaled zone and the outer zone are of order R/L and ϵ, but there is no difference of order $Pr_{ref}M^2/\epsilon$. Similar considerations, but to order $Pr_{ref}M^2/\epsilon$, apply with respect to the transverse velocities and the boundary conditions given by $(8, h, l)$.

Taking (14), (15), and respectively (17) and (18) into account, one finds that

$$\left.\frac{\mathrm{d}p_{12}}{\mathrm{d}x}\right|_0 = -8\gamma \frac{\mu(T_L)}{\mu_{ref}} U_L \tag{19}$$

and

$$\left.\frac{\mathrm{d}p_{12}}{\mathrm{d}x}\right|_1 = -8\gamma \frac{\mu(T_R)}{\mu_{ref}} U_R; \tag{20}$$

$$u_0 = 2T_0(r^2 - 1)\left(\frac{1}{p_0}\frac{\mathrm{d}p_0}{\mathrm{d}t}\int_0^x \frac{1}{T_0}\,\mathrm{d}x - \frac{U_L}{T_L}\right). \tag{21}$$

The global mass flow rate over the entire cross-section is given by

$$\dot{m}_0 = \pi\left(p_0 \frac{U_L}{T_L} - \frac{\mathrm{d}p_0}{\mathrm{d}t}\int_0^x \frac{1}{T_0}\,\mathrm{d}x\right). \tag{22}$$

The leading-order flow field is now determined except for $T_0(x)$. In an initial value problem, $T_0(x)$ would be fully determined by the initial conditions. Thus, at this stage, any arbitrary temperature profile would provide a valid solution.

The pressure gradient can be determined, replacing u_0 in (14) by (21):

$$\frac{\partial p_{12}}{\partial x} = 8\gamma \frac{\mu(T_0)}{\mu_{ref}} T_0\left(\frac{1}{p_0}\frac{\mathrm{d}p_0}{\mathrm{d}t}\int_0^x \frac{1}{T_0}\,\mathrm{d}x - \frac{u_L}{T_L}\right). \tag{23}$$

Boundary conditions for p_{12} are obtained from the continuity equation of order $Pr_{ref}M^2/\epsilon$:

$$\frac{\partial \rho_{12}}{\partial t}+\frac{\partial(\rho_0 u_{12}+\rho_{12}u_0)}{\partial x}+\frac{1}{r}\frac{\partial(\rho_0 v_{12}r+\rho_{12}v_0 r)}{\partial r}=0. \tag{24}$$

Integrating over the entire cross-section, the last term vanishes. From $(6g,k)$, the velocity $u_{12}=0$ at $x=0$ and $x=1$, since the entire non-homogeneous velocity boundary conditions, which are of leading order, have already been included in the leading-order boundary condition u_0 given by (17) and (18), and since the corrections due to the inner, entry length region, by virtue of being of order ϵ and R/L, but not $Pr_{ref}M^2/\epsilon$, do not contribute to u_{12}, which is thus 0. Integrating over the whole tube length and taking into account also that $p_{12}=\rho_0 T_{12}+\rho_{12}T_0$, with T_{12} zero throughout since the problem for T_{12} is homogeneous so that $p_{12}=T_0\rho_{12}$, one obtains

$$\int_0^1 \frac{\partial \rho_{12}}{\partial t}\,\mathrm{d}x+\frac{p_{12,R}U_R}{T_R}-\frac{p_{12,L}U_L}{T_L}=0, \tag{25}$$

$$\frac{\mathrm{d}}{\mathrm{d}t}\int_0^1 \rho_{12}\,\mathrm{d}x+(p_{12,R}-p_{12,L})\frac{U_R}{T_R}+p_{12,L}\left(\frac{U_R}{T_R}-\frac{U_L}{T_L}\right)=0. \tag{26}$$

ρ_{12} is independent of r, since p_{12} is according to $(13b)$, and $p_{12}/p_0=\rho_{12}/\rho_0$. Also, the last term in (26) can be replaced from (10). Thus

$$\bar{T}\int_0^1 \frac{\mathrm{d}p_{12}}{T_0\,\mathrm{d}t}\,\mathrm{d}x-p_{12,L}\frac{1}{p_0}\frac{\mathrm{d}p_0}{\mathrm{d}t}=-\bar{T}(p_{12,R}-p_{12,L})\frac{U_R}{T_R}, \tag{27}$$

and p_{12} is obtained by integrating (23):

$$p_{12}=p_{12,L}+8\gamma\frac{1}{p_0}\frac{\mathrm{d}p_0}{\mathrm{d}t}\int_0^x\left(T_0\frac{\mu(T_0)}{\mu_{ref}}\int_0^x\frac{1}{T_0}\mathrm{d}x\right)\mathrm{d}x-8\gamma\frac{U_L}{T_L}\int_0^x T_0\frac{\mu(T_0)}{\mu_{ref}}\mathrm{d}x, \tag{28}$$

$$p_{12,R}-p_{12,L}=8\gamma\frac{1}{p_0}\frac{\mathrm{d}p_0}{\mathrm{d}t}\int_0^1 T_0\left(\frac{\mu(T_0)}{\mu_{ref}}\int_0^x\frac{1}{T_0}\mathrm{d}x\right)\mathrm{d}x-8\gamma\frac{U_L}{T_L}\int_0^1 T_0\frac{\mu(T_0)}{\mu_{ref}}\mathrm{d}x. \tag{29}$$

Substituting p_{12} from (28), and $p_{12,R}-p_{12,L}$ from (29), into (27), the following equation is obtained:

$$\begin{aligned}\frac{p_0}{8\gamma\bar{T}}\frac{\mathrm{d}}{\mathrm{d}t}\left(\frac{p_{12,L}}{p_0}\right)=&-\frac{\mathrm{d}^2\log p_0}{\mathrm{d}t^2}\int_0^1\left(\frac{1}{T_0}\int_0^x\left(T_0\frac{\mu(T_0)}{\mu_{ref}}\int_0^x\frac{1}{T_0}\mathrm{d}x\right)\mathrm{d}x\right)\\&\times\mathrm{d}x+\frac{\mathrm{d}U_L}{T_L\,\mathrm{d}t}\int_0^1\left(\frac{1}{T_0}\int_0^x T_0\frac{\mu(T_0)}{\mu_{ref}}\mathrm{d}x\right)\mathrm{d}x-\frac{\mathrm{d}p_0}{p_0\,\mathrm{d}t}\int_0^1\left(T_0\frac{\mu(T_0)}{\mu_{ref}}\int_0^x\frac{1}{T_0}\mathrm{d}x\right)\\&\times\mathrm{d}x+\frac{U_R U_L}{T_R T_L}\int_0^1 T_0\frac{\mu(T_0)}{\mu_{ref}}\mathrm{d}x.\end{aligned} \tag{30}$$

Integration of (30) yields the left-hand boundary value of p_{12}. Finally, (29) determines the value of p_{12} at the right-hand end. Both values are determined up to an absolute integration constant, which is all that is needed to evaluate the viscous losses.

5.4. *Problem of order* ϵ

To leading order, $(6d)$, the energy equation for the fluid, led to a gas temperature that was uniform in the transverse direction. The next non-trivial perturbation to that energy equation is smaller by a factor ϵ, so that the transverse temperature gradients are of order ϵ.

One complication arises, however, from the continuity conditions at the gas–wall interface: both temperatures and heat fluxes are continuous. Replacing T and T_m by their perturbation series in (6r), continuity of the heat flux implies that at $r = 1$ or, equivalently, at $\sigma = R/d$:

$$\frac{k(T_0+\epsilon T_{11}+\ldots)}{k_{ref}}\frac{\partial(\delta T_0+\epsilon\delta T_{11}+\delta^2 T_{13}+\epsilon^2\delta T_{21}\ldots)}{\partial r}$$

$$= a(T_0+\epsilon T_{m11}+\ldots)\frac{\partial(\epsilon T_{m0}+\epsilon^2 T_{m11}+\epsilon\delta T_{m13}+\epsilon^3 T_{m21}+\epsilon^2\delta T_{m23}+\ldots)}{\partial\sigma} \quad (31)$$

so that, at the interface,

$$\left.\frac{\partial T_{m11}}{\partial\sigma}\right|_{\sigma=R/d} = 0 \quad \text{and} \quad \left.\frac{k(T_0)}{k_{ref}}\frac{\partial T_{11}}{\partial r}\right|_{r=1} = a(T_0)\left.\frac{\partial T_{m13}}{\partial\sigma}\right|_{\sigma=R/d}, \quad (32a, b)$$

but also, from (8r),

$$T_{11}(x, l, t) = T_{m11}(x, R/d, t) \quad \text{and} \quad T_{13}(x, l, t) = T_{m13}(x, R/d, t). \quad (33a, b)$$

At the interface, the gas temperatures of order ϵ match values also of order ϵ for the wall, while the transverse temperature gradient of order ϵ in the gas must be matched to the gradient of order δ in the wall. Therefore, the problem of order ϵ for the gas is related to both problems, of order ϵ and δ, for the wall.

The wall problem of order ϵ includes

$$\frac{\partial T_{m11}}{\partial t} = a(T_0)\frac{1}{\sigma}\frac{\partial(\sigma\,\partial T_{m11}/\partial\sigma)}{\partial\sigma}, \quad (34)$$

which is the perturbation of order ϵ to (6e), with Neumann boundary conditions given by (32a), and by the perturbation to (6s):

$$\left.\frac{\partial T_{m11}}{\partial\sigma}\right|_{\sigma=1+R/d} = 0. \quad (35)$$

It is a problem in σ and t with homogeneous boundary conditions, in which x enters only as a parameter. Its unique stationary or periodic solution is $T_{m11} = T_{m11}(x)$.

The problem of order ϵ for the gas temperature, which, because of continuity of the heat flux vector, is coupled with the problem of order δ for the wall, can be described by the following equations, obtained by collecting terms of order ϵ in the relevant equations (6) with the values for pressure, temperatures, density and velocities replaced from (7):

$$\frac{1}{\gamma}\frac{\partial(\rho_0 T_0)}{\partial t}+\frac{1}{r}\frac{\partial(rv_0 p_0)}{\partial r}+\frac{\partial(u_0 p_0)}{\partial x} = \frac{k(T_0)}{k_{ref}}\frac{1}{r}\frac{\partial(r\,\partial T_{11}/\partial r)}{\partial r}, \quad (36a)$$

$$\frac{\partial T_{m13}}{\partial t} = a(T_0)\frac{1}{\sigma}\frac{\partial(\sigma\,\partial T_{m13}/\partial\sigma)}{\partial\sigma}, \quad (36b)$$

$$T_{11}(x, l, t) = T_{m11}(x), \quad (36c)$$

$$\left.\frac{k(T_0)}{k_{ref}}\frac{\partial T_{11}}{\partial r}\right|_{r=1} = a(T_0)\left.\frac{\partial T_{m13}}{\partial\sigma}\right|_{\sigma=R/d}, \quad (36d)$$

$$\left.\frac{\partial T_{m13}}{\partial\sigma}\right|_{\sigma=1+R/d} = 0, \quad (36e)$$

$$T_{11}(0, r, t) = T_{m11}(0, r, t) = 0 \quad \text{when} \quad u_0(0, r, t) > 0, \quad (36f)$$

$$T_{11}(l, r, t) = T_{m11}(l, r, t) = 0 \quad \text{when} \quad u_0(l, r, t) < 0. \quad (36g)$$

u_0 and v_0 are replaced (in 36a) by their values from (21) and (16), and after integration of the result, the value of $\partial T_{11}/\partial r$ is obtained; at the wall, for $r = 1$, it is given by

$$\frac{k(T_0)}{k_{ref}}\frac{\partial T_{11}}{\partial r} = \frac{p_0}{2}\frac{U_L}{T_L}\frac{dT_0}{dx} - \frac{1}{2}\frac{dp_0}{dt}\left(\frac{dT_0}{dx}\int_0^x \frac{1}{T_0}dx + \frac{\gamma-1}{\gamma}\right). \tag{37}$$

After a second integration, the value of T_{11} in the field is found, given by

$$\frac{k(T_0)}{k_{ref}}T_{11} = \frac{r^4-4r^2+3}{8}\frac{dT_0}{dx}\left(\frac{dp_0}{dt}\int_0^x \frac{1}{T_0}dx - \frac{p_0 U_L}{T_L}\right) - (r^2-1)\frac{\gamma-1}{4\gamma}\frac{dp_0}{dt} + \frac{k(T_0)}{k_{ref}}T_{m11}(x), \tag{38}$$

noting that, by virtue of (36c), at $r = 1$, $T_{11} = T_{m11}$ which depends upon x only.

The temperature scale T_{ref} was chosen arbitrarily. But the dimensional value that can be reconstructed from T_{11} given by (38) is well-defined, because the product ϵT_{ref} is independent of that arbitrary value T_{ref}. Indeed, α is proportional to k divided by density, and thus proportional to T_{ref}, so that ϵ is inversely proportional to T_{ref}. The magnitude of the temperature perturbation is then found as

$$T' \approx \epsilon T_{ref}\frac{k_{ref}}{k(T_0)} = \frac{P_{ref}R^2}{\tau k(T_0)}\frac{\gamma}{\gamma-1}.$$

5.5. *Problem of order* ϵ^2

So far, to order ϵ, all variables are unconditionally periodic, and all energy fluxes are unconditionally balanced over one full revolution. The highest order at which energy transfers occur which are not inherently balanced for arbitrary $T_0(x)$ is ϵ^2, and the corresponding energy equation for the fluid is

$$\frac{1}{\gamma}\frac{\partial p_{11}}{\partial t} + \frac{1}{r}\frac{\partial(rv_0 p_{11} + rv_{11}p_0)}{\partial r} + \frac{\partial(u_0 p_{11} + u_{11}p_0)}{\partial x} = \frac{k(T_0)}{k_{ref}}\frac{1}{r}\frac{\partial\left(r\dfrac{\partial T_{21}}{\partial r}\right)}{\partial r} + \frac{1}{k_{ref}}\frac{dk(T_0)}{dT}T_{11}\frac{1}{r}\frac{\partial\left(r\dfrac{\partial T_{11}}{\partial r}\right)}{\partial r}, \tag{39a}$$

which is the perturbation of order ϵ^2 to (6d). The continuity condition for the heat flux at the interface, given by (31) – see §5.4 above – relates the flux of order ϵ^2 in the fluid to the flux of order $\epsilon\delta$ in the wall, and can be written as

$$\frac{k(T_0)}{k_{ref}}\frac{\partial T_{21}}{\partial r}\bigg|_{r=1} + \frac{1}{k_{ref}}\frac{dk(T_0)}{dT}T_{11}\frac{\partial T_{11}}{\partial r}\bigg|_{r=1} = a(T_0)\frac{\partial T_{m23}}{\partial \sigma}\bigg|_{\sigma=R/d} + T_{11}\frac{da}{dT}\bigg|_{T_0}\frac{\partial T_{m13}}{\partial \sigma}\bigg|_{\sigma=R/d}. \tag{39b}$$

The corresponding energy equation for the wall is thus of order $\epsilon\sigma$, and it is given by

$$\frac{\partial T_{m23}}{\partial t} - b(T_0)\frac{\partial^2 T_{m0}}{\partial x^2} = a(T_0)\left\{\frac{1}{\sigma}\frac{\partial\left(\sigma\dfrac{\partial T_{m23}}{\partial r}\right)}{\partial \sigma}\right\} + T_{11}\frac{da}{dT}\bigg|_{T_0}\left\{\frac{1}{\sigma}\frac{\partial\left(\sigma\dfrac{\partial T_{m13}}{\partial r}\right)}{\partial \sigma}\right\}. \tag{39c}$$

Finally,

$$\frac{\partial T_{m23}}{\partial \sigma}\bigg|_{\sigma=1+R/d} = 0. \tag{39d}$$

The problem of order ϵ^2 provides the condition ensuring that energy transfers are balanced, so that the solution is periodic. The overall energy balance is obtained by integration over the entire cross-sections. The details are as follows. Integrating (39*a*) multiplied by $2\pi r\,\mathrm{d}r$, with respect to r, between 0 and 1, and (39*c*) multiplied by $2\pi\sigma\,\mathrm{d}\sigma$ through the pipe wall, for σ from R/d to $1+R/d$, two equations are obtained which, in view of (36*e*) and (39*b*), have opposite right-hand sides, up to a factor R/d. Eliminating the right-hand sides, integrating with respect to time over a full period, and taking into account that the solution is periodic in time, and that $T_{m0} = T_0$, one obtains

$$\int_0^1 \mathrm{d}t \int_0^1 \left(\frac{\partial(u_0 p_{11} + u_{11} p_0)}{\partial x} \right) 2\pi r\,\mathrm{d}r - \pi(2 + d/R) \frac{\mathrm{d}}{\mathrm{d}x}\left(b(T_0) \frac{\mathrm{d}T_0}{\mathrm{d}x} \right) = 0. \tag{40}$$

Replacing $p_{11} = \rho_0 T_{11} + \rho_{11} T_0$ and $p_0 = \rho_0 T_0$ in the first term of (40), and noting that T_0 is independent of t and r, it follows that

$$\frac{\mathrm{d}}{\mathrm{d}x}\left(\int_0^1 \mathrm{d}t \int_0^1 u_0 \rho_0 T_{11}\, 2\pi r\,\mathrm{d}r - b\pi(2 + d/R) \frac{\mathrm{d}T_0}{\mathrm{d}x} + T_0 \int_0^1 \mathrm{d}t \int_0^1 (u_0 \rho_{11} + u_{11} \rho_0)\, 2\pi r\,\mathrm{d}r \right) = 0. \tag{41}$$

The second integral in (41) vanishes, since it is an expression for the net mass flow rate of order ϵ over one full period. Integrating (41) with respect to x, defines the quantity H_{11}:

$$H_{11} = \int_0^1 \mathrm{d}t \int_0^1 u_0 \rho_0 T_{11}\, 2\pi r\,\mathrm{d}r - b(T_0)\,\pi(2 + d/R) \frac{\mathrm{d}T_0}{\mathrm{d}x}, \tag{42}$$

which represents the energy transferred along the tube over one period. This quantity is usually referred to as the *enthalpy flux*, following an original suggestion by Wheatley *et al.* (1983). At the periodic regime, it is uniform lengthwise, hence an absolute constant. ($H_0 = 0$ since T_0 is time independent and $\rho_0 u_0$ is periodic.) Replacing $u_0 \rho_0$ and T_{11} by their values as functions of T_0 and using the mass flow rate $\dot{m}_0(x, t)$ given by (22), the enthalpy flux can be written as

$$H_{11} = \int_0^1 \mathrm{d}t\,\mathrm{d}t \int_0^1 (r^2 - 1) \frac{k_{ref}}{k(T_0)} \dot{m}_0 \left(\frac{r^4 - 4r^2 + 3}{2\pi} \frac{\mathrm{d}T_0}{\mathrm{d}x} \dot{m}_0 + (r^2 - 1) \frac{\gamma - 1}{\gamma} \frac{\mathrm{d}p_0}{\mathrm{d}t} \right) \times r\,\mathrm{d}r - b(T_0)\,\pi(2 + d/R) \frac{\mathrm{d}T_0}{\mathrm{d}x}. \tag{43}$$

Finally, the integrals with respect to r are computed:

$$H_{11} = \frac{-11}{48\pi} \frac{k_{ref}}{k(T_0)} \frac{\mathrm{d}T_0}{\mathrm{d}x} \int_0^1 \dot{m}_0^2\,\mathrm{d}t + \frac{\gamma - 1}{6\gamma} \frac{k_{ref}}{k(T_0)} \int_0^1 \dot{m}_0 \frac{\mathrm{d}p_0}{\mathrm{d}t}\,\mathrm{d}t - b(T_0)\,\pi(2 + d/R) \frac{\mathrm{d}T_0}{\mathrm{d}x}. \tag{44}$$

If, in (44), $\dot{m}_0$ is replaced by its value from (22), and p_0 by its value from (11), a first order integro-differential equation for T_0 is obtained. Two boundary conditions are available, since temperatures are known at both ends. The problem is not overdetermined, however. In (44), the absolute constant H_{11} is unknown, and furthermore, through p_0, (44) also depends upon $\bar{T}$, also an absolute constant, given as a function of the solution T_0 by (12), and initially also unknown. In effect, both H_{11} and $\bar{T}$ appear as eigenvalues. Equation (44) shows that three components contribute to the enthalpy flux. The first term corresponds to a contribution that always goes in the direction opposite to the temperature gradient. It is proportional to the mean value of

the square of the mass flow rate $\dot{m}_0$, and it exists and is non-zero even if pressure is uniform. The second term, which is non-zero only if there is a pressure fluctuation and to the extent that pressure and mass flow rate are out of phase, *can contribute a flux against the temperature gradient, i.e. reversible heat pumping*. The third term represents the contribution of conduction in the wall.

When the mass flow rates at both ends are equal at all times, then, according to (10), the leading-order pressure remains constant. (Because of the near-isothermal assumption, temperature fluctuations are too small to result in leading-order pressure changes.) Equation (44) shows that the longitudinal temperature gradient is then uniform, even if longitudinal conduction in the wall is significant, provided that the thermal conductivity of the wall, hence b, is temperature independent.

Equation (44) shares the main features of the result obtained in a similar one-dimensional near-isothermal model (Bauwens (1995) in which a convection coefficient from an empirical correlation between Reynolds number and Nusselt number was used. For laminar flow in a straight tube, the Nusselt number for uniform heat flux equals 48/11. Using that value for the Nusselt number, the one-dimensional model yields the enthalpy flux given by

$$H_{1D} = \frac{-11}{48\pi}\frac{k_{ref}}{k(T_0)}\frac{\mathrm{d}T_0}{\mathrm{d}x}\int_0^1 \dot{m}_0^2\,\mathrm{d}t + \frac{11}{48}\frac{\gamma-1}{\gamma}\frac{k_{ref}}{k(T_0)}\int_0^1 \dot{m}_0\frac{\mathrm{d}p_0}{\mathrm{d}t}\,\mathrm{d}t - b\pi(2+d/R)\frac{\mathrm{d}T_0}{\mathrm{d}x}. \quad (45)$$

This shows that the one-dimensional model does not evaluate correctly the contribution of the pressure swing to the enthalpy flux, which it overestimates by a factor 11/8, or 37.5%, in the case of laminar flow in a tube.

Both Thomann (1976) and Rott (1975) have proposed expressions similar to (44), respectively for tubes larger and smaller than the Stokes layer, but for the *local* enthalpy flux. These studies considered the case of arbitrary, unbalanced wall temperatures, within the scenario of incipient Taconis waves, in which the wall temperature, hence the net heat stored in the wall, is changing, so that, in contrast with the current solution, their enthalpy flux is not uniform lengthwise.

6. Tube closed at one end

Rott (1984) has paid particular attention to the problem in which one end of the tube is closed. The end at $x = 0$ is now blind, so that $U_L = 0$. In the limit case when longitudinal conduction in the wall is negligible ($b = 0$), the mass flow rate given by (22) becomes

$$\dot{m}_0 = -\pi\frac{\mathrm{d}p_0}{\mathrm{d}t}\int_0^x \frac{1}{T_0(x)}\,\mathrm{d}x, \quad (46)$$

which shows that velocities are now in phase throughout the length. The enthalpy flux is

$$H_{11} = -\pi\frac{k_{ref}}{k(T_0)}\left(\frac{11}{48}\frac{\mathrm{d}T_0}{\mathrm{d}x}\int_0^x \frac{1}{T_0}\,\mathrm{d}x + \frac{\gamma-1}{6\gamma}\right)\int_0^x \frac{1}{T_0}\,\mathrm{d}x\int_0^1 \left(\frac{\mathrm{d}p_0}{\mathrm{d}t}\right)^2\mathrm{d}t. \quad (47)$$

Since the factor between brackets on the right-hand side of (47) has a finite limit for $x \to 0$, while if the total mass of fluid in the tube is finite, the factor $\int_0^x (1/T_0)\,\mathrm{d}x \to 0$, H_{11} is necessarily zero. This is because there is no longer any physical mechanism present in the model that could remove energy from the left-hand end. Indeed, longitudinal conduction in the wall and in the fluid have now been neglected, and at $x = 0$ velocity is always zero, so that there is no convection either.

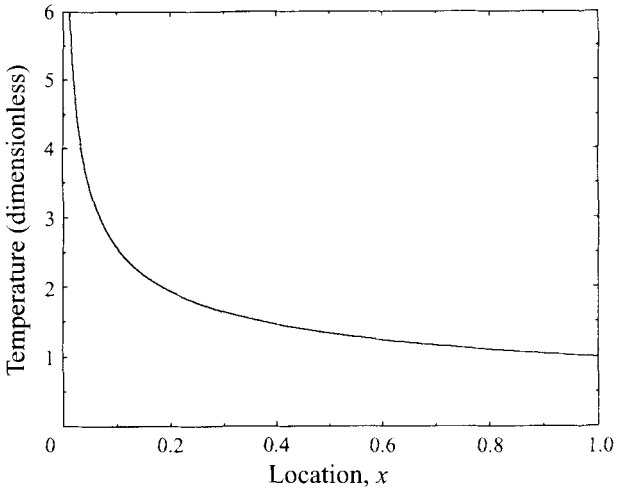

FIGURE 2. Tube closed at left-hand end – longitudinal temperature profile T/T_R.

However, away from $x = 0$, the last two integrals in (47) are not zero, except in the trivial case where p_0 is uniform. Thus, since H_{11}, being uniform lengthwise, is zero throughout the length, the factor between brackets necessarily vanishes, so that the temperature profile is determined by the differential equation

$$\frac{11}{48}\frac{\mathrm{d}T_0}{\mathrm{d}x}\int_0^x \frac{1}{T_0}\,\mathrm{d}x + \frac{\gamma-1}{6\gamma} = 0. \tag{48}$$

Integration by parts of the first term, followed by integration of the whole equation, results in

$$T_0\int_0^x \frac{1}{T_0}\,\mathrm{d}x = \left(1-\frac{8(\gamma-1)}{11\gamma}\right)x, \tag{49}$$

which can be integrated again, yielding

$$\bar{T}\int_0^x \frac{1}{T_0}\,\mathrm{d}x = x^{11\gamma/(3\gamma+8)} \tag{50}$$

and, finally,

$$T_0 = \frac{(3\gamma+8)}{11\gamma}\bar{T}x^{-8(\gamma-1)/(3\gamma+8)}. \tag{51}$$

That a left-hand temperature boundary condition can no longer be imposed should come as no surprise, since physically there no longer is any fluid entering from the left, so that the original problem no longer supports a left-hand temperature boundary condition. Taking into account that at $x = 1$, $T_0 = T_R$, one finds

$$T_0 = T_R x^{-8(\gamma-1)/(3\gamma+8)}, \tag{52}$$

$$\bar{T} = 11\gamma T_R/(3\gamma+8). \tag{53}$$

Knowing $\bar{T}$, p_0 is determined by (11), u_0 by (21) and v_0 by (16), thus completing the solution. Figure 2 shows the temperature profile as given by (52), for helium ($\gamma = 5/3$). Pressure gradients can readily be calculated by numerical integration of (29) and (30).

These results show that the leading-order temperature T_0 exhibits a singularity at the closed end, $x = 0$. The magnitude assumptions break down near $x = 0$ and a different

distinguished limit involving some of the terms which have been neglected, such as longitudinal conduction, becomes applicable in a narrow zone, limiting the temperature to a finite value.

A detailed solution in the case where $b \neq 0$ can be obtained following the same procedure as in the next section, setting $J = 0$. A system in which a heat exchanger or an adiabatic volume is placed at the closed end can also be analysed following the procedure in the next section. In all these cases, the mass flow rate remains in phase with $\mathrm{d}p_0/\mathrm{d}t$. But since H_{11} is no longer zero, (47) no longer simplifies to (48).

Rott (1984) found an identical behaviour for the singularity that occurs at the closed end of a tube, with same exponent, equal to $-8(\gamma-1)/(3\gamma+8)$, also in narrow tubes. The current result is thus a generalization of Rott's for high pressure amplitudes, but for shorter tubes.

It is a pleasant surprise that for this problem of a tube closed at one end, the one-dimensional near-isothermal model with empirical convection coefficient, but assuming flow passages smaller than the Stokes layer thickness, yields an exponent equal to $1-\gamma$ (Bauwens 1995), which is the same value obtained for tubes larger than the Stokes layer thickness, according to an argument originally proposed by Gifford & Longsworth (1966) and discussed by Rott (1984) and Wheatley *et al.* (1983). This is because the one-dimensional model and Gifford & Longsworth's argument share the assumption that the fluid temperature is spatially uniform in the transverse direction, except possibly for a discontinuity at the wall. Thus, their argument holds also for the assumptions embedded in the one-dimensional model, in which the only role of the assumption of thick Stokes layer is to ensure that it is nearly isothermal.

The two models differ significantly in another respect. Physically, the key to both models is energy conservation for the temperature perturbation T_{11}, which is given here by

$$\frac{1-\gamma}{\gamma}\frac{\mathrm{d}p_0}{\mathrm{d}t}+\rho_0 u_0\frac{\mathrm{d}T_0}{\mathrm{d}x}+\frac{1}{r}\frac{\partial(rv_0 p_0)}{\partial r}=\frac{k(T_0)}{k_{ref}}\frac{1}{r}\frac{\partial\left(r\dfrac{\partial T_{11}}{\partial r}\right)}{\partial r}, \tag{54}$$

obtained from (36*a*). Equation (54) shows that there is a balance between longitudinal convection, changes in internal energy, transverse convection, and transverse conduction.

Irreversibilities only occur in this model because of conduction in the transverse direction. But the following equation

$$\frac{k(T_0)}{k_{ref}}T_{11}=-\frac{\mathrm{d}p_0}{\mathrm{d}t}(1-4r^2)(1-r^2)\frac{\gamma-1}{44\gamma}+\frac{k(T_0)}{k_{ref}}T_{m11}(x), \tag{55}$$

obtained by specializing (38) to the case of tubes closed at one end, shows that T_{11} has a non-zero transverse gradient, even though since the enthalpy flux equals zero, its average value, weighted by $\rho_0 u_0$, is equal to T_{m11} (see (42), setting $b = 0$ and $H_{11} = 0$) and, obviously, its value at the wall is also equal to T_{m11}. *Thus, there is irreversible conduction in the transverse direction in the fluid even with zero net enthalpy flux. In contrast, the one-dimensional model simply results in* $T_{11} = T_{m11}(x)$: there is no discontinuity at the wall. That model cannot differentiate the mean, mass-averaged temperature from the value at the wall. The bulk temperature of the fluid is then equal to the wall temperature in the one-dimensional model, which effectively results in a reversible solution, when the correct two-dimensional solution shows that it is not.

7. Tube open at both ends

A solution similar to that obtained in the previous section can also be obtained in the case of non-zero velocity boundary conditions at both ends. This solution applies for example to tubular regenerators, or to a tube with a closed volume, such as, for example, a heat exchanger, at the end.

As above for tubes closed at one end, in the solution that follows, longitudinal conduction in the wall is again neglected, and b is set equal to zero. (A solution including conduction in the wall would only require a slight modification in the definition of the constant K, below.) Additionally, the thermal conductivity k of the fluid is assumed to be temperature independent. (For temperature-dependent k, equation (66) below cannot be integrated in closed form; but a numerical solution can still readily be implemented using a similar procedure.)

The strategy is similar to the previous section, but an iterative solution is now required. Again, $\dot{m}_0$ is replaced by its value from (22) in the enthalpy flux equation, (44), which is then solved for T_0 and the eigenvalue H_{11}. It is convenient to rewrite the problem in terms of $f(x)$ defined by

$$f(x) = \bar{T}\int_0^x \frac{1}{T_0(x)}\,\mathrm{d}x, \tag{56}$$

instead of $T_0(x)$, thus eliminating the integral of $1/T_0$ and transforming (44) into a straightforward, if nonlinear, ordinary differential equation.

For simplicity the following notation is introduced. The coefficients defined by

$$I = \int_0^1 \left(\frac{\mathrm{d}p_0}{\bar{T}\,\mathrm{d}t}\right)^2 \mathrm{d}t, \tag{57}$$

$$J = \int_0^1 \frac{\mathrm{d}p_0}{\bar{T}\,\mathrm{d}t} p_0 \frac{u_L}{T_L}\,\mathrm{d}t, \tag{58}$$

$$K = \int_0^1 \left(p_0 \frac{u_L}{T_L}\right)^2 \mathrm{d}t, \tag{59}$$

are time-integrals over one full revolution of quantities that depend upon $p_0(t)$ and the velocities at the ends, but are independent of x. Consequently, they are absolute constants, but unknown since they depend upon $\bar{T}$. The quadratic form $If^2 - 2Jf + K$ is then given by

$$If^2 - 2Jf + K = \int_0^1 \left(f\frac{\mathrm{d}p_0}{\bar{T}\,\mathrm{d}t} - p_0\frac{u_L}{T_L}\right)^2 \mathrm{d}t = \frac{1}{\pi^2}\int_0^1 \dot{m}_0^2\,\mathrm{d}t \tag{60}$$

Rewriting (44) in terms of $f(x)$, and using the newly defined parameters I, J and K, (44) is transformed into

$$\bar{T}H_{11} = \frac{11\pi}{48}(If^2 - 2Jf + K)\frac{f''}{f'^2} - \frac{\pi}{6}\frac{\gamma - 1}{\gamma}(If - J). \tag{61}$$

a second-order ordinary differential equation for f. Besides $f(x)$, (61) contains two additional unknowns, the absolute constants $\bar{T}$ and H_{11}, which must be counted as two

separate unknowns because I, J and K also depend upon $\bar{T}$, independently of H_{11}. But there are four boundary conditions:

$$\text{At} \quad x=0, \quad f=0 \quad \text{and} \quad \frac{\mathrm{d}f}{\mathrm{d}x}=\frac{\bar{T}}{T_L}, \tag{62a, b}$$

$$\text{At} \quad x=1, \quad f=1 \quad \text{and} \quad \frac{\mathrm{d}f}{\mathrm{d}x}=\frac{\bar{T}}{T_R}. \tag{62c, d}$$

In principle, the problem is thus determined. Equation (61) can be rearranged as follows:

$$\frac{f''}{f'}=\frac{48\bar{T}H_{11}/11\pi+\frac{8}{11}(\gamma-1)/\gamma(If-J)}{If^2-2Jf+K}f'. \tag{63}$$

Integrating between 0 and f and taking into account the boundary conditions at $x=0$,

$$T_L f'=\bar{T}\left(\frac{If^2-2Jf+K}{K}\right)^{4(\gamma-1)/11\gamma} \times\exp\left(\frac{48\bar{T}H_{11}}{11\pi(KI-J^2)^{1/2}}\left(\arg\tan\frac{If-J}{(KI-J^2)^{1/2}}+\arg\tan\frac{J}{(KI-J^2)^{1/2}}\right)\right). \tag{64}$$

The quadratic form $If^2-2Jf+K$ is a sum of exact squares. Its roots are complex except if the integrand in (60) vanishes for a value of f that is time independent, in which case the double root is $f=J/I$. In that case, for reasons similar to those seen above in the closed tube at $x=0$, $H_{11}=0$ and, from (64), $f'=0$ at the location where $f(x)=J/I$ so that the local temperature goes to infinity at that location. However, except for a phase angle between velocities at the ends equal to 180° (see below), the quadratic form is strictly positive, thus avoiding the singularity. Integrating (63) between $x=0$ and $x=1$, $\bar{T}H_{11}$ is obtained:

$$\bar{T}H_{11}=\frac{11\pi(KI-J^2)^{1/2}}{48}\frac{\left(\log(T_L/T_R)-\frac{4(\gamma-1)}{11\gamma}\log\left(\frac{I-2J+K}{K}\right)\right)}{\arg\tan\frac{I-J}{(KI-J^2)^{1/2}}+\arg\tan\frac{J}{(KI-J^2)^{1/2}}}. \tag{65}$$

Finally, integrating (64) between 0 and x, gives

$$\int_0^f\left(\frac{If^2-2Jf+K}{K}\right)^{-4(\gamma-1)/11\gamma} \times\exp\left(\frac{-48\bar{T}H_{11}}{11\pi(KI-J^2)^{1/2}}\left(\arg\tan\frac{If-J}{(KI-J^2)^{1/2}}+\arg\tan\frac{J}{(KI-J^2)^{1/2}}\right)\right)\mathrm{d}f=\frac{x\bar{T}}{T_L}, \tag{66}$$

which gives $f(x)$ implicitly, and integrating the same equation between 0 and 1, gives

$$\int_0^1\left(\frac{If^2-2Jf+K}{K}\right)^{-4(\gamma-1)/11\gamma} \times\exp\left(\frac{-48\bar{T}H_{11}}{11\pi(KI-J^2)^{1/2}}\left(\arg\tan\frac{If-J}{(KI-J^2)^{1/2}}+\arg\tan\frac{J}{(KI-J^{21/2}}\right)\right)\mathrm{d}f=\frac{\bar{T}}{T_L}, \tag{67}$$

which determines $\bar{T}$. However, I, J, and K depend upon $\bar{T}$, which is unknown initially, so that a technique such as, for instance, an iterative numerical solution starting with

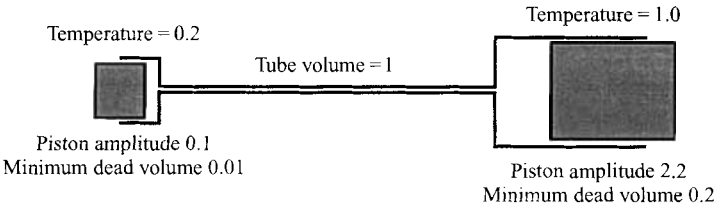

FIGURE 3. Geometry.

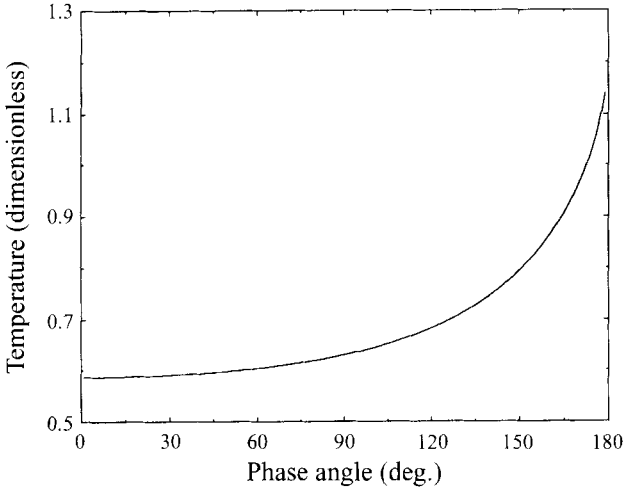

FIGURE 4. Tube open at both ends – mean temperature, as defined by equation (12), *vs.* phase angle.

a guessed value of $\bar{T}$ and eventually converging to a fixed point is required. But here, a procedure based upon a systematic search is implemented. A range large enough to contain all possible solutions for $\bar{T}$ is divided into small intervals. The intervals within which a solution exists are those over which the difference between the guessed value and the calculated value changes sign.

The results below correspond to the geometry of figure 3, for a temperature ratio 1:5 (for instance 65 K/325 K), and for helium ($\gamma = 5/3$). The piston motion is sinusoidal, with amplitudes equal to 0.1 and 2.2 and dead volumes to mid-stroke equal to 0.11 and 2.4 times the volume of the tube. The phase angle between pistons ranges from 0 to 180°. Temperatures in the cylinders are constant, which implies that the cylinders are in thermal contact with a heat source or sink at the appropriate temperature. This geometry actually describes a refrigerator; it was chosen because it is equivalent to a geometry used in the previous study with a one-dimensional approximation (Bauwens 1995, high pressure amplitude case).

Figure 4 shows how $\bar{T}$ varies with the phase angle. Figure 5 shows the reversible leading-order refrigeration (equal to the leading-order work done at the cold end, since the leading-order enthalpy flux is zero) and the dimensionless enthalpy flux H_{11}, of order ϵ, *vs.* phase angle. The scalars by which the leading-order refrigeration and H_{11} must be multiplied to recover dimensional values in Watts are respectively $\pi P R^2 L$ and $\gamma^2 P^2 R^4 L/(\gamma-1)^2 \tau k T_R$. (These results cannot be translated into global performance data such as coefficient of performance or ineffectiveness, except for specific values of the scalars. Likewise, Hausen's (1929) concepts of reduced length and reduced

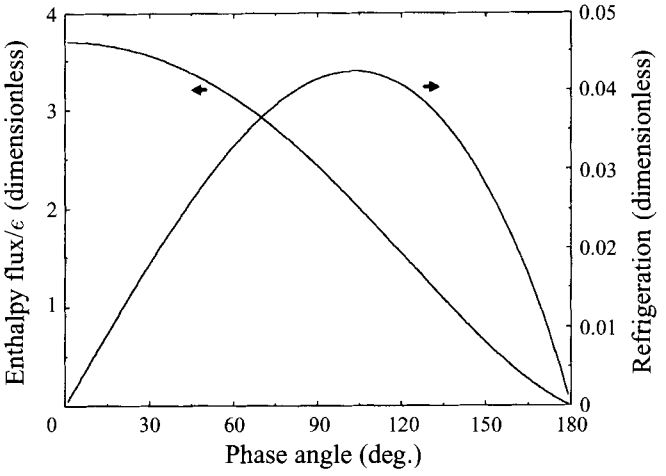

FIGURE 5. Tube open at both ends – dimensionless enthalpy flux/ϵ and refrigeration *vs.* phase angle.

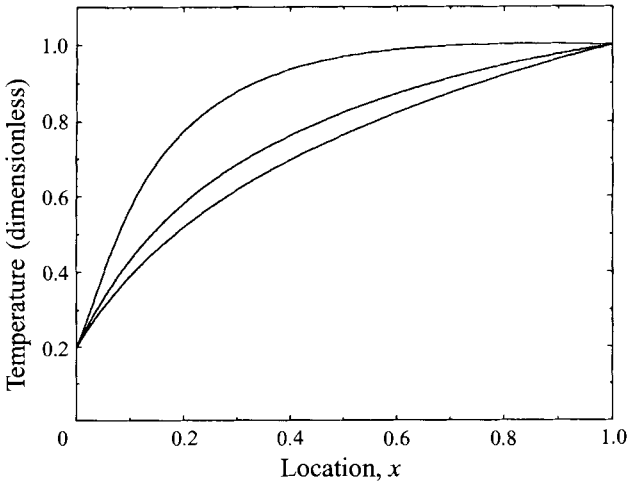

FIGURE 6. Tube open at both ends – longitudinal temperature profiles at 45°, 90° and 135° phase angles (higher curve corresponds to a larger phase angle).

frequency (also in Schmidt & Willmott 1981) do not apply, because heat transfer is not based upon a constant empirical convection coefficient but evaluated from first principles, and because the mass flow rates at the extremities are time dependent.) Figure 6 shows temperature profiles for three values of the phase angle.

Figure 7 shows that, as the phase angle approaches 180°, the solution exhibits a sharp spike approaching infinity in the temperature. At 180°, velocities and mass flow rates at the ends are in opposite phases, and according to (11), pressure is then in phase with the largest of the mass flow rates at the ends. The mass flow rate no longer has a phase that shifts with position along the length. Instead, the tube can be divided into two parts, in each of which the mass flow rate is in phase with the mass flow rate at the end. At the location x^* separating the two regions, the mass flow rate remains zero throughout the period. The quadratic form $If^2+2Jf+K$ defined by (60) is then a perfect square and its zero, $f=J/I$, defines the value of $f(x^*)$ at the interface x^*. In effect, each side operates as if a rigid boundary existed at x^*, and each side can be

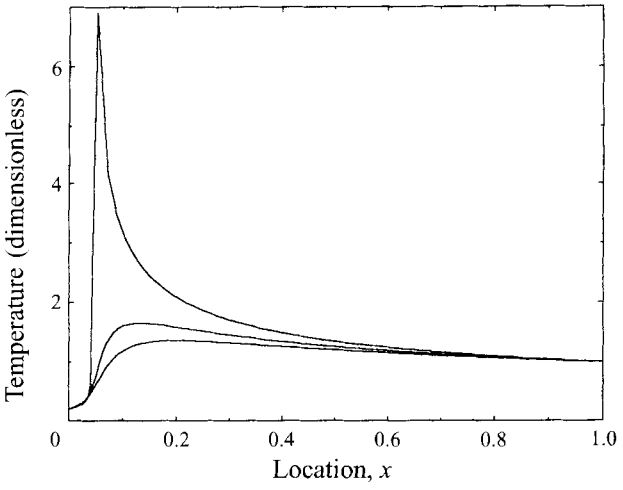

FIGURE 7. Tube open at both ends – longitudinal temperature profiles at 170°, 175° and 180° phase angles (higher curve corresponds to a larger phase angle – at 180° peak truncated to a finite value because of numerical inaccuracy).

described as a tube closed at one end. Thus, a singularity occurs at x^*, of the type previously described for tubes closed at one end. H_{11} is zero and the temperature goes to infinity at x^*. (On figure 7, however, the peak remains finite at 180° because of numerical inaccuracy).

Except in the neighbourhood of 180° when effects of pressure fluctuations become more significant, the numerical results are virtually identical to results obtained previously using the one-dimensional model (Bauwens 1995) in which the term representing the effect of pressure fluctuation in (44) was overstated by a factor 11/8 for round tubes. Thus the effect of pressure fluctuation does not appear to be very significant in regenerators.

Finally, while no results were presented for the pressure gradient, it is worth mentioning that the solution also determines the viscous losses. Indeed, once $\bar{T}$, $T_0(x)$ and $p_0(t)$ have been found, it is straightforward to integrate (30) and (29) numerically, and to calculate the contribution of order $Pr\,M^2/\epsilon$ to the pressure fluctuations at both ends. If $Pr\,M^2$ is larger than ϵ^2, these losses can be larger than the enthalpy flux.

8. Enthalpy flux and pulse-tube refrigeration

It is clear that the theory applies to regenerators. Indeed, while the leading-order enthalpy flux is zero, in the general case studied, with non-zero velocities at both ends, there is a non-zero, uniform entropy flux moving along the tube. This is equivalent to a 'work' flux and a 'heat' flux moving along the tube, both of same magnitude, equal to the entropy flux times the local temperature, but moving in opposite directions. The energy fluxes are thus balanced at both ends, i.e. the work absorbed equals the heat released at each end. This describes the ideal Stirling refrigerator, in which the reversible regenerator merely moves a uniform entropy flux from one end to the other, resulting in the Carnot efficiency. That the theory also describes basic pulse-tube refrigeration is perhaps not so obvious.

In the absence of a heat exchanger or, as in the basic pulse-tube, of the piston at one extremity, because the leading-order work and heat fluxes are necessarily balanced at the ends and one of them is now zero, so is the other. As a result, the leading-order

entropy flux vanishes too and all leading order fluxes are thus necessarily zero. The enthalpy flux of order ϵ, H_{11}, becomes the largest non-zero energy flux. If, in (44), the term in $\int \dot{m}_0 \, dp_0$ is positive and larger than the terms that depend upon the temperature gradient, H_{11} goes in the direction from the cold end to the warm end.

If H_{11} is larger than the work done by the piston at the cold end, then there is net refrigeration. This heat pumping mechanism relies upon periodic exchange between work from pressure forces and heat stored in the wall. It crucially depends upon the phase relationship between pressure and mass flow rate, which varies along the tube. This is fundamentally the same heat streaming effect originally identified by Gifford & Longsworth (1968), studied by Rott (1975) and Merkli & Thomann (1975), and also described by de Boer (1994, 1995).

In the first case above, of a tube closed at one end, the two main terms in (44) were found to be non-zero, but they exactly balanced each other, leading to a zero overall enthalpy flux H_{11}. If a heat exchanger is added at the warm end, limiting the local temperature to a finite value, then H_{11} is no longer zero. If appropriate conditions are met, resulting in an entropy flux leaving at the warm end larger than the total entropy produced, net refrigeration occurs. If the heat exchanger placed at the warm end has a sizable dead volume, though, and even if the fluid in the heat exchanger is assumed to remain at a fixed wall temperature, this system then falls within the realm of the second case above, in which velocities are non-zero at both tube ends. Indeed, while the detailed results shown above considered a configuration with pistons at both ends, the solution developed in the second case, which merely assumes that the velocities are non-zero at the ends, remains valid and unchanged even if $\int_0^1 u_0 p_0 \, dt = 0$ at one end, so that all leading-order fluxes vanish and H_{11} becomes the largest non-zero flux.

But the main goal of the current study was to establish the basic theory. An investigation of that particular configuration and, more generally, of the basic pulse-tube, which may also include the regenerator, will require some additional issues to be dealt with, however. This includes matching between the regenerator, in which the quantity $d^2/\alpha\tau$, based upon the mesh size, is typically indeed very small, and the pulse-tube, in which the assumption of small ϵ will probably not be so accurate, so that in effect, these two zones are best dealt with using two independent perturbation schemes. In a study of the complete device, boundary conditions will require a different treatment, since the velocities at the interfaces can no longer be imposed, but they depend upon the overall configuration. Perhaps more significantly, complete performance evaluation will require not only the enthalpy flux to be evaluated, but also the entropy flux, so as to allow for a division of the enthalpy flux into heat and work at the tube ends. This is dealt with in a separate study that builds upon the current theory, but targets specifically the basic pulse-tube refrigerator, with a freezer at the cold end, and in configurations with or without regenerator (Bauwens 1996).

Finally, considering pulse-tube refrigeration in the small-tube limit, it is clear that, generally, the enthalpy flux includes a reversible component. And since the same fundamental mechanism is responsible for both the enthalpy leaking through a regenerator and for pulse-tube refrigeration, then typically, in regenerators also, there should be a reversible component in the enthalpy flux, which is thus not entirely a loss. However, one of the conclusions of the second case studied in detail above was that the effect of the pressure fluctuation term in (44) was minimal in regenerators. This seems to indicate that the reversible component will usually not be very significant.

9. Conclusions

A closed-form approximate solution to the periodic, two-dimensional, oscillating flow boundary value problem with heat transfer and large pressure swings in a cylindrical tube was developed, with viscous stresses and heat transfer based upon the appropriate laws of molecular diffusion, avoiding empirical convective heat transfer and friction coefficients.

The perturbation solution determines the enthalpy flux and the longitudinal temperature profile attained in the periodic regime, thus resolving the indeterminacy of the isothermal Schmidt model. Key to the solution is the requirement that the small but non-zero total longitudinal enthalpy flux, which appears as a small perturbation to the isothermal solution, must be uniform along the tube length. That requirement can be translated into an integro-differential equation for the time-independent leading-order temperature, which remained arbitrary in the isothermal solution.

The current solution determines the uniform enthalpy flux at equilibrium, and the corresponding equilibrium temperature distribution. This contrasts with the work of Rott (1975) and Thomann (1976), who also investigated the enthalpy flux in periodic flow, although in a longer tube and for smaller pressure amplitudes, but whose analysis was limited to initial, arbitrary temperature profiles, in which case the flux varies lengthwise.

Results were presented for two configurations: with one end closed and with two open ends. The first configuration is a classical problem, for which a closed-form expression for the temperature distribution was found. The second configuration corresponds to tubular regenerators. The assumptions made accurately reflect regenerators in Stirling and possibly in some pulse-tube refrigerators. The model determines the entropy flux (hence, in the case of regenerators, the leading-order refrigeration), the enthalpy flux and the pressure gradients and associated losses, which are possibly even larger than the enthalpy flux, thus fully characterizing the performance of the device.

Results from the model show that:

(i) In a tube closed at one end, a temperature singularity occurs at the closed end. The temperature profile is given by a power-law relationship with longitudinal position. The exponent, valid for arbitrary pressure amplitudes, is the same as found by Rott (1984) for small pressure amplitudes;

(ii) In tubes open at both ends, when the mass flow rates at the ends are of opposite phases, the temperature may go to infinity at a location inside the tube where the velocity remains zero throughout the period. That singularity is similar to the one observed at closed ends;

(iii) One-dimensional models with empirical convection coefficients (Nusselt numbers) yield results that, according to this study, are correct only for tubes larger than the thermal layer, even in the case of laminar flow in a tube smaller than the thermal layer;

(iv) The current theory contains the basic physics of basic pulse-tube refrigeration, albeit in the narrow limit.

We thank Professor Nicholas Rott for his encouragement and for his penetrating comments. Work supported by the Natural Sciences and Engineering Research Council of Canada.

REFERENCES

BAUWENS, L. 1995 The near-isothermal regenerator: a perturbation analysis. *J. Thermophys. Heat Transfer* **9**, 749–756.

BAUWENS, L. 1996 Entropy balance and performance characterization of the narrow basic pulse-tube refrigerator. *J. Thermophys. Heat Transfer* (in press).

BAUWENS, L. & MITCHELL, M. P. 1991 Regenerator analysis: validation of the MS*2 Stirling cycle code. In *Proc. XVIIIth Intl Congress of Refrigeration*, vol. III, pp. 930–934. International Institute of Refrigeration Paris.

BOER, P. C. T. DE 1994 Thermodynamic analysis of the basic pulse-tube refrigerator. *Cryogenics* **3**, 699–712.

BOER, P. C. T. DE 1995 Analysis of basic pulse-tube refrigerator with regenerator. *Cryogenics* **35**, 547–553.

GARY, J. & RADEBAUGH, R. 1989 A numerical model for regenerator performance [REGEN 3]. Interim Report for Period May 1987 December 1988. *Flight Dynamics Laboratory, Wright–Patterson AFB, Rep.* WRDC-TR-89-3049.

GEDEON, D. R. 1986 A globally-implicit Stirling cycle simulation. *Proc. 21st Intersociety Energy Conversion Engineering Conference, ACS, Washington, DC*, pp. 550–556.

GIFFORD, W. E. & LONGSWORTH, R. C. 1964 Pulse-tube refrigeration. *Trans ASME* B: *J. Engng Indust.* **86**, 264–268.

GIFFORD, W. E. & LONGSWORTH, R. C. 1966 Surface heat pumping. *Adv. Cryogenic Engng* **11**, 171–179.

GU, Y. & TIMMERHAUS, K. D. 1994 Experimental verification of stability characteristics for thermal acoustic oscillations in a liquid helium system. *Adv. Cryogenic Engng* **39B**, 1733–1740.

HAUSEN, H. 1929 Über die Theorie des Wärmeaustausches in Regeneratoren. *Z. Angew. Math. Mech.* **9**, 173–200.

KIRCHHOFF, G. 1868 Über den Einfluss der Wärmeleitung in einem Gas auf die Schallbewegungen. *Ann. Phys. Leipzig* (2) **134**, 177–193.

KITTEL, P. 1992 Ideal orifice pulse tube refrigerator performance. *Cryogenics* **32**, 843–844.

KRAMERS, H. A. 1949 Vibrations of a gas column. *Physica* **15**, 971–984.

LEE, J. M., KITTEL, P., TIMMERHAUS, K. D. & RADEBAUGH, R. 1995 Steady secondary momentum and enthalpy streaming in the pulse tube refrigerator. In *Cryocoolers 8* (ed. R. J. Ross), pp. 359–369. Plenum.

MERKLI, P. & THOMANN, H. 1975 Thermoacoustic effects in a resonance tube. *J. Fluid Mech.* **70**, 161–177.

MIRELS, H. 1994*a* Effect of orifice flow and heat transfer on gas spring hysteresis. *AIAA J.* **32**, 1656–1661.

MIRELS, H. 1994*b* Linearized theory for pulse tube cryocooler performance. *AIAA J.* **32**, 1662–1669.

MÜLLER, U. A. & ROTT, N. 1983 Thermally driven acoustic oscillations, Part VI: Excitation and power. *Z. Angew. Math. Phys.* **34**, 610–626.

OLSON, J. R. & SWIFT, G. W. 1994 Similitude in thermoacoustics. *J. Acoust. Soc. Am.* **95**, 1405–1412.

ORGAN, A. J. 1992 *Thermodynamics and Gas Dynamics of the Stirling Cycle Machine*. Cambridge University Press.

QVALE, E. B. & SMITH, J. L., JR 1969 An approximate solution for the thermal performance of a Stirling-engine regenerator. *Trans. ASME* A: *J. Engng Power* **2**, 109–112.

RADEBAUGH, R. 1990 A review of pulse tube refrigeration. *Adv. Cryog. Engng* **35**, 1191–1206.

RAYLEIGH, LORD 1896 *Theory of Sound*, 2nd Edn, vol. 2, Mcmillan.

REA, S. N. & SMITH, J. L., JR 1967 The influence of pressure cycling on thermal regenerators. *Trans. ASME* B: *J. Engng Indust.* **89**, 563–569.

ROTT, N. 1969 Damped and thermally driven acoustic oscillations in wide and narrow tubes. *Z. Angew. Math. Phys.* **20**, 230–243.

ROTT, N. 1973 Thermally driven acoustic oscillations, Part II: Stability limits for helium. *Z. Angew. Math. Phys.* **24**, 54–72.

ROTT, N. 1975 Thermally driven acoustic oscillations, Part III: Second order heat flux. *Z. Angew. Math. Phys.* **26**, 43–49.

ROTT, N. 1984 Thermoacoustic heating at the closed end of an oscillating gas column. *J. Fluid Mech.* **145**, 1–9.

ROTT, N. & ZOUZOULAS, G. 1976 Thermally driven acoustic oscillations, Part IV: Tubes with variable cross-section. *Z. Angew. Math. Phys.* **27**, 197–224.

RUDMAN, I. KH. 1994 Flow rate instabilities under self-sustained cooling. *Cryogenics* **34**, 555–562.

SCHMIDT, F. W. & WILLMOTT, A. J. 1981 *Thermal Energy Storage and Regeneration.* Hemisphere.

SCHMIDT, G. 1871 Theorie der Lehmann'schen kalorische Maschine. *Z. Vereins Deutsch. Ing.* **15**, No. 1, 1–12.

SPRENGER, H. 1954 Über die thermische Effekte in Resonanzrohren. *Mitt. I.f.A.E., Eidgenössische Technische Hochschule, Zürich*, No. 21, p. 18.

STORCH, P. J. & RADEBAUGH, R. 1988 Development and experimental test of an analytical model of the orifice pulse tube refrigerator. *Adv. Cryo. Engng* **33**, 851–859.

SWIFT, G. W. 1988 Thermoacoustic engines. *J. Acoust. Soc. Am.* **84**, 1145.

SWIFT, G. W. & WARD, W. C. 1995 Simple harmonic analysis of stacked-screen regenerators. *Los Alamos National Laboratory Rep.* LA-UR-95-1577; also *J. Thermophys. Heat Transfer* (submitted).

TACONIS, K. W., BEENAKKER, J. J. M., NIER, A. O. C. & ALDRICH, L. T. 1949 Measurements concerning the Vapour–Liquid Equilibrium of Solutions of He^3 in He^4 below 2.19 K. *Physica* **15**, 733–739.

THOMANN, H. 1976 Acoustic streaming and thermal effects in pipe flow with high viscosity. *Z. Angew. Math. Phys.* **27**, 709–715.

URIELI, I. & BERCHOWITZ, D. M. 1984 *Stirling engine Analysis.* Bristol: Adam Hilger.

WEST, C. 1993 Some single-piston closed-cycle machines and Peter Tailer's thermal lag engine. In *Proc. 28th IECEC, American Chemical Society*, vol. 2, pp. 673–679.

WHEATLEY, J., HOFLER, T., SWIFT, G. W. & MIGLIORI, A. 1983 An intrinsically irreversible thermoacoustic heat engine. *J. Acoust. Soc. Am.* **74**, 153–170.

ZOUZOULAS, G. & ROTT, N. 1976 Thermally driven acoustic oscillations, Part V: Gas–Liquid oscillations. *Z. Angew. Math. Phys.* **27**, 326–334.